

## ANALYSIS OF WAVEFORM RETRACKING METHODS IN ANTARCTIC ICE SHEET BASED ON CRYOSAT-2 DATA

XIAO Feng<sup>a,b</sup> LI Fei<sup>a,b,\*</sup> ZHANG Shengkai<sup>a,b,\*</sup> HAO Weifeng<sup>a,b</sup> YUAN Lexian<sup>a,b</sup> ZHU Tingting<sup>c</sup> ZHANG Yu<sup>a,b</sup>  
ZHU Chaohui<sup>a,b</sup>

<sup>a</sup> Chinese Antarctic Center of Surveying and Mapping, Wuhan University, Wuhan 430079, China

<sup>b</sup> Collaborative Innovation Center for Territorial Sovereignty and Maritime Rights, Wuhan 430079, China

<sup>c</sup> State Key Laboratory of Information Engineering in Surveying, Mapping and Remote Sensing, Wuhan University, Wuhan  
430079, China

**KEY WORDS:** CryoSat-2; waveform retracking; Antarctic; ice sheet; satellite altimetry

### ABSTRACT:

Satellite altimetry plays an important role in many geoscientific and environmental studies of Antarctic ice sheet. The ranging accuracy is degenerated near coasts or over nonocean surfaces, due to waveform contamination. A postprocess technique, known as waveform retracking, can be used to retrack the corrupt waveform and in turn improve the ranging accuracy. In 2010, the CryoSat-2 satellite was launched with the Synthetic aperture Interferometric Radar ALtimeter (SIRAL) onboard. Satellite altimetry waveform retracking methods are discussed in the paper. Six retracking methods including the OCOG method, the threshold method with 10%, 25% and 50% threshold level, the linear and exponential 5- $\beta$  parametric methods are used to retrack CryoSat-2 waveform over the transect from Zhongshan Station to Dome A. The results show that the threshold retracker performs best with the consideration of waveform retracking success rate and RMS of retracking distance corrections. The linear 5- $\beta$  parametric retracker gives best waveform retracking precision, but cannot make full use of the waveform data.

### 1. INTRODUCTION

Satellite altimetry is used to detect the earth and its variation precisely and periodically on a large scale. The satellite altimetry data are widely used to study the earth gravity field model, mean sea level, oceanic tidal model and seabed topography. In Polar Regions, satellite altimetry has proven to be a valuable tool for many geoscientific and environmental studies. It can, for example, be used for ice sheet mapping and mass balance study (Bamber et al. 2009, Zhang et al. 2015, Li et al. 2016). It is also used to detect sea ice changes in polar areas (Yuan et al. 2016).

However, the echo waveforms of altimetry impulse are often contaminated by the coastal terrain, islands,

oceanic tide, geophysical conditions and hardware delay over nonocean areas. This kind of waveform is so irregular that the distance between the altimetry satellite and its nadir point cannot be precisely estimated from the waveforms. In order to calculate precise distances, the middle point of waveform leading edge should be repositioned, then the distance correction should be reestimated by comparing the retracked middle point of leading edge and the pre-given gate, which is called the waveform retracking technique of radar satellite altimetry.

The European Space Agency's (ESA) satellite CryoSat-2, launched in April 2010, carries a radar altimeter named Synthetic aperture Interferometric Radar Altimeter

\* Corresponding author (fli@whu.edu.cn)

(SIRAL) (Wingham et al 2006). CryoSat-2 provides altimetry data up to a latitude of 88° S/N, which is a significant improvement to previous satellite borne altimeters. The narrow across-track spacing of 2.5 km at 70° and 4 km at 60° deliver high data coverage at the margins of the ice sheet. This is an improvement compared to the coarse across-track spacing of 25 km at 70° and 40 km at 60° of the ICESat. In addition to the dense track spacing and the smaller data gap around the South Pole, CryoSat-2 also features the high accuracy in sloped terrain due to the newly developed SIRAL instrument. This capability is a significant improvement compared to the conventional altimeters on board ERS1/2/ENVISAT and enables continuous observations along the relatively steep and narrow margins of the ice sheets as well as on large glaciers and ice caps, where elevation change is most rapid.

Different waveform retracking techniques have been developed for altimeter measurements over ice sheets (Martin et al. 1983; Wingham et al. 1986; Davis 1997). Waveform retracking methods have been compared over coastal and deep ocean (Guo et al. 2006; Lee et al. 2010; Khaki et al. 2014). The purpose of this study is to evaluate waveform retracking methods in Antarctic by retracking the CryoSat-2 waveforms. We applied six retracking algorithms including the Off Center of Gravity (OCOG), the threshold retracking method with 10%, 25% and 50% threshold level respectively, the linear and exponential 5-β parametric method to the CryoSat-2 return waveforms over the transect from Zhongshan Station to Dome A.

## 2. WAVEFORM RETRACKING TECHNIQUE

Methods of waveform retracking can be classified into two categories: one is based on functional fit and the other based on statistics.

### 2.1 OCOG algorithm

In 1986, Wingham et al. put forward the OCOG algorithm, which is a simple waveform retracking method based on the statistical characteristics of waveforms. The center of gravity of waveform should be firstly searched, then the waveform amplitude, width and

position of center of gravity should be estimated with the numerical method, seeing Figure 1. The method is very simple, but not correlative to the physical characteristics of returned surface. The equations of OCOG are as follows:

$$COG = \frac{\sum_{n=1+aln}^{n=N-aln} ny^2(n)}{\sum_{n=1+aln}^{n=N-aln} y^2(n)} \quad (1)$$

$$A = \sqrt{\frac{\sum_{n=1+aln}^{n=N-aln} y^4(n)}{\sum_{n=1+aln}^{n=N-aln} y^2(n)}} \quad (2)$$

$$W = \frac{\left( \sum_{n=1+aln}^{n=N-aln} y^2(n) \right)^2}{\sum_{n=1+aln}^{n=N-aln} y^4(n)} \quad (3)$$

$$Lep = COG - 0.5W \quad (4)$$

where  $N$  is the total gate number;  $aln$  is the number of eliminated gate in the starting and ending of waveform;  $y(n)$  is the power of the  $n^{\text{th}}$  gate;  $A$  is the amplitude;  $W$  is the width;  $COG$  is the center of gravity of waveform;  $LEP$  is the middle point of leading edge.

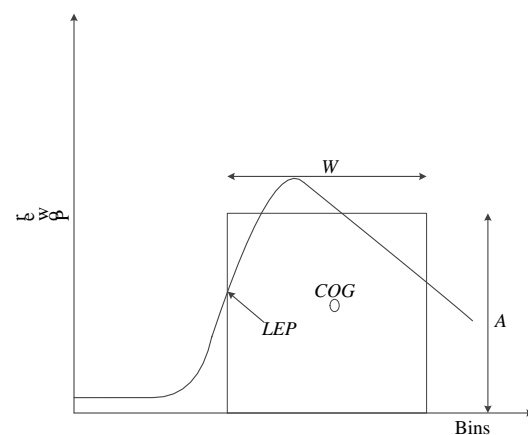


Figure 1. Schematic diagram of the OCOG algorithm

### 2.2 Threshold algorithm

Davis put forward the threshold algorithm to retrack altimetry waveforms in 1997. The threshold level should be determined based on the amplitude and the maximum waveform power calculated with OCOG. The retracked point can be obtained to linearly interpolate the neighboring samples close to the intersecting threshold

between the threshold level and the leading edge. The threshold method is a statistical method and not of physical characteristics. The method can give more precise retracking gate than OCOG. The corresponding equations are as follows:

$$y_N = \frac{1}{5} \sum_{i=1}^5 y(i) \quad (5)$$

$$T_L = y_N + T_h(A - y_N) \quad (6)$$

$$\begin{cases} n_{ret} = (k-1) + \frac{T_L - y(k-1)}{y(k) - y(k-1)} & y(k) \neq y(k-1) \\ n_{ret} = (k-1) & y(k) = y(k-1) \end{cases} \quad (7)$$

where  $y(i)$  is the power of  $i^{\text{th}}$  gate;  $y_N$  is the average power of former 5 gates;  $T_L$  is the threshold level;  $A$  is the amplitude;  $k$  is the  $k^{\text{th}}$  gate whose power is more than  $T_L$ ;  $n_{ret}$  is the middle point of leading edge.

### 2.3 $\beta$ parametric fitting algorithm

The  $\beta$  parametric fitting algorithm was firstly put forward by Martin et al. in 1983 from the National Aeronautics and Space Administration, USA (NASA). The method uses a relevant parametric function to fit the altimetry waveform based on the Brown mean impulse echo model. B parameters can be estimated by the iterative calculation based on good initial values with the least squares adjustment or the maximum likelihood estimator. The 5- $\beta$  parametric method is mainly used to process the complex waveform returned from the single reflecting surface, shown in Figure 2. If the waveform is present like a spike, the 5- $\beta$  parametric algorithm may be non-convergent in the iterative procedure and cannot give the right results. The linear 5- $\beta$  parametric equation is:

$$y(t) = \beta_1 + \beta_2(1 + \beta_5 Q(t)) P\left(\frac{t - \beta_3}{\beta_4}\right) \quad (8)$$

$$P(z) = \frac{1}{\sqrt{2\pi}} \int_{-\infty}^z e^{-\frac{q^2}{2}} dq = \frac{1}{2} + \frac{1}{2} \operatorname{erf}\left(\frac{z}{\sqrt{2}}\right) \quad z = \frac{t - \beta_3}{\beta_4} \quad (9)$$

$$Q(t) = \begin{cases} 0 & t < \beta_3 + 0.5\beta_4 \\ t - (\beta_3 + 0.5\beta_4) & t \geq \beta_3 + 0.5\beta_4 \end{cases} \quad (10)$$

Where  $y(t)$  is the sampling power at time  $t$ ;  $\beta_1$  is the thermal noise of returned waveform;  $\beta_2$  is the returned impulse power for leading edge;  $\beta_3$  is the middle point of leading edge which is the half power from the received power to the maximum power and used to

calculate the difference to the pre-given gate and get the retracking distance correction;  $\beta_4$  is the risetime parameter;  $\beta_5$  is the slope of ramping edge;  $P(z)$  is the error function;  $Q(t)$  is a linear function to fit the gradual attenuation echo wave in the ramping edge.

The exponential 5- $\beta$  parametric equation is:

$$y(t) = \beta_1 + \beta_2 e^{-\beta_5 Q(t)} P\left(\frac{t - \beta_3}{\beta_4}\right) \quad (11)$$

$$P(z) = \frac{1}{\sqrt{2\pi}} \int_{-\infty}^z e^{-\frac{q^2}{2}} dq = \frac{1}{2} + \frac{1}{2} \operatorname{erf}\left(\frac{z}{\sqrt{2}}\right) \quad z = \frac{t - \beta_3}{\beta_4} \quad (12)$$

$$Q(t) = \begin{cases} 0 & t < \beta_3 - 2\beta_4 \\ t - (\beta_3 - 2\beta_4) & t \geq \beta_3 - 2\beta_4 \end{cases} \quad (13)$$

The 5 parameters  $\beta_i$  in the algorithm can be estimated with the least squares method. But the selection of unknown-parameter initial values and the determination of sampling power weight are important to get the optimal results. In this study, the method to give the initial values of unknown parameters and determine the weight is the same as that Anzenhofer et al. (1999) have used to process ERS-1 waveforms.

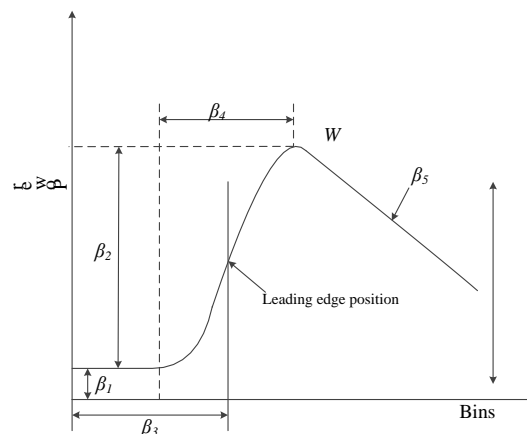


Figure 2. Schematic diagram of 5- $\beta$  parameter method

### 2.4 Retracking distance correction

After retracking waveforms, the middle point of leading edge can be determined. According to the pre-given gate and the light velocity, the retracking distance correction  $\Delta R$  is:

$$\Delta R = 0.5 t_k c (n_{ret} - n_r) \quad (14)$$

where  $t_k$  is the time interval for one gate;  $c$  is the light velocity,  $c=299792458$  m/s;  $n_{ret}$  is the middle point of leading edge; and  $n_r$  is the pre-given gate.

## 3. DATA AND METHOD

### 3.1 CryoSat-2 data and study areas

The CryoSat-2 satellite was launched on April 8, 2010, carrying a new developed altimeter operating in Ku-band. The SIRAL instrument samples the surface every 300 m along track using three different measurement modes, LRM, SAR and SARIn. The low resolution mode (LRM) is used over oceans and the flat interior of the ice sheets. LRM is similar to the operation of conventional pulsedwidth-limited altimeters. In the synthetic aperture (SAR) and synthetic aperture interferometric (SARIn) modes, SIRAL samples the surface with a higher pulse repetition frequency (18 181 Hz) than in LRM (1970 Hz). SARIn measures the steep areas at the margins of the ice sheet and ice caps, whereas the SAR mode is used over sea ice to reveal ice free-board by distinguishing leads and ice flows.

In this study, we use the CryoSat-2 LIB product provided by ESA, which contains the precise orbit of the satellite, the back-scattered radar waveforms, the tracker range and the coherence and phase difference for SARIn mode. The product also contains additional information, such as geophysical and tidal corrections and quality flags.

Figure 3 shows the study areas with CryoSat-2 ground tracks over the transect from Zhongshan Station to Dome A. This area is the core area of the Chinese Antarctic Scientific Expedition (Zhang, et al. 2007, 2008). We investigate the CryoSat-2 waveforms collected in December 2013 in this study. In this area, the LRM and SARIn mode are adopted over interior and margins of the ice sheet respectively.

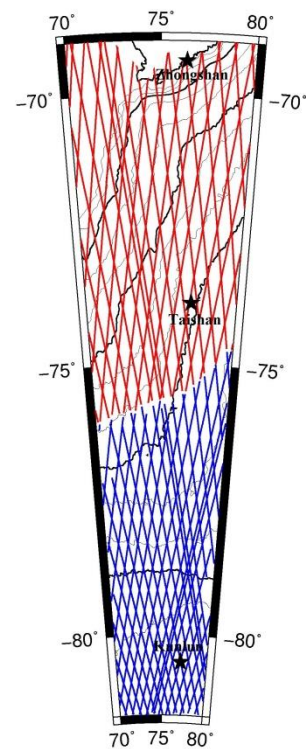


Figure 3. Ground tracks for CryoSat-2 over the transect from Zhongshan Station to Dome A, the blue lines indicate the LRM tracks, while the red lines indicate the SARIn tracks.

### 3.2 Waveform retracking

Six waveform retracking methods including the OCOG retracker, the threshold retracker with 10%, 25%, 50% threshold level, the linear and exponential  $5-\beta$  retracker were used to retrack Cryosat-2 waveforms. The mean and RMS of retracking distance correction and the success rate of are calculated for LRM and SARIn waveforms, respectively. The results are shown in Table 1. The waveform retracking success rate and the RMS of retracking distance correction are used to assess impacts of waveform retracking methods. The retracking success rate is the ratio of retracking waveform number and total waveform number.

	LRM			SARIn		
	Mean/m	RMS/m	Success rate	Mean/m	RMS/m	Success rate
OCOG	-2.119	2.009	100%	250.261	148.636	100%
Threshold-10%	-3.933	2.457	100%	129.504	130.469	100%
Threshold -25%	-2.753	2.193	100%	178.621	115.875	100%

Threshold -50%	-1.247	1.977	100%	224.289	135.435	100%
Linear 5- $\beta$	-0.218	1.655	92.3%	215.047	103.757	76.2%
Exponential 5- $\beta$	-0.109	1.548	22.1%	—	—	0.6%

Table 1. Statistics of waveform retracking results

The success rates for LRM waveforms are 92.3% and 22.1% with the two 5- $\beta$  parametric fitting methods. The success rates for the other retracking methods are all 100%. The RMSs from the two 5- $\beta$  parametric methods are low, which indicates that the two methods can give good retracking results. The RMS for threshold method is the minimum when the threshold is 50%. Figure 4 is the histograms of retracking results for LRM waveforms, the gray line indicates the onboard tracking point. The retracking results from the two 5- $\beta$  parametric methods and the threshold method with 50% threshold level are close to normal distribution.

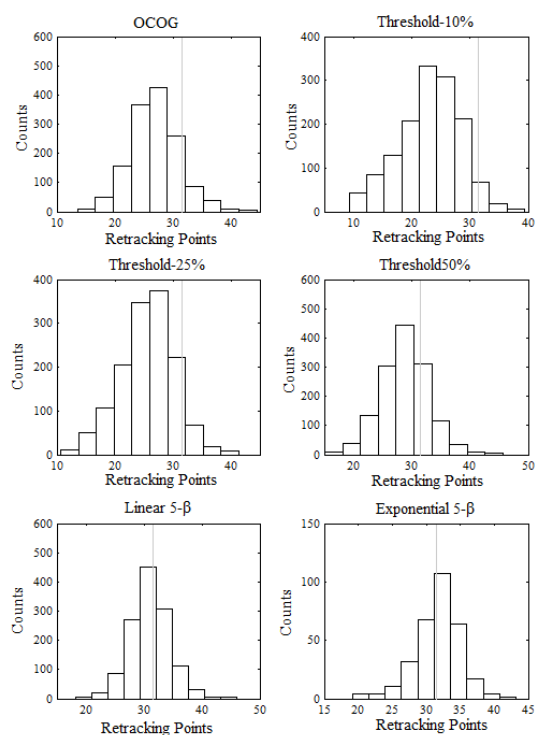


Figure 4. Histograms of retracking results for LRM waveforms, the gray line indicates the pre-given gate.

The success rate for SARIn waveforms is too low with the exponential 5- $\beta$  parametric fitting method and results of retracking distance corrections are not calculated. The success rate for the linear 5- $\beta$  parametric method is 76.2%. The RMSs for the linear 5- $\beta$  parametric and threshold method with 25% threshold level are low among the five retracking methods. Figure 5 is the

histograms of retracking results for SARIn waveforms. The distribution of the results from five retracking methods is discrete.

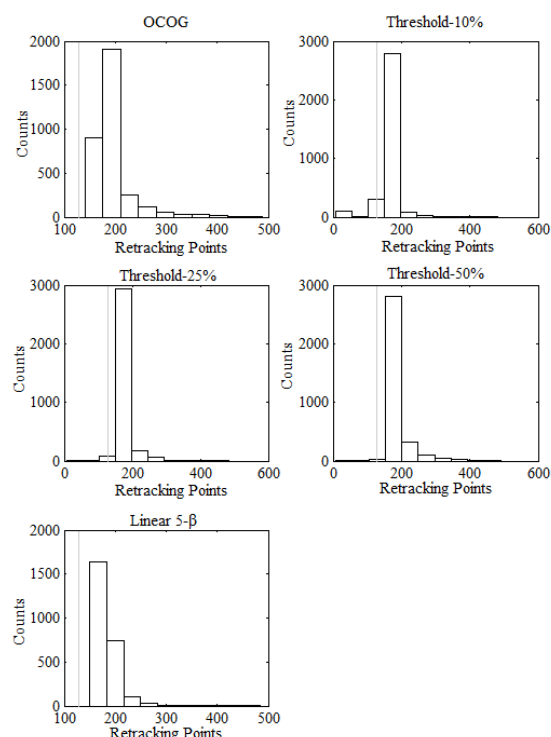


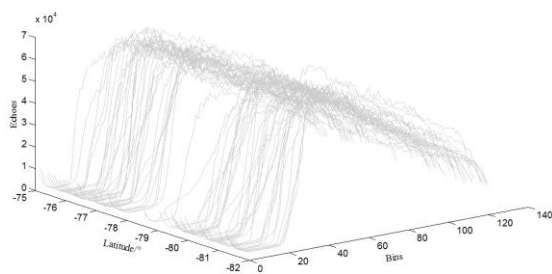
Figure 5. Histograms of retracking results for SARIn waveforms, the gray line indicates the pre-given gate.

#### 4. DISCUSSIONS

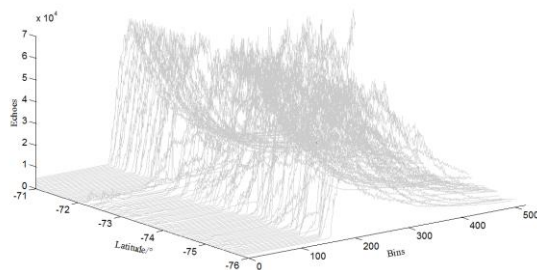
According to the comparison, the linear 5- $\beta$  parametric fitting algorithm outperforms other methods for both two types of waveforms. But the 5- $\beta$  parametric method is much more complex and needs a longtime computation. Moreover, the 5- $\beta$  parametric method cannot make full use of all the waveforms because of infinite iterations during the least squares calculation. The OCOG and threshold method are based on statistics and have no definite physical meaning. These two methods have the advantages of fast calculating speed and full data utilization. OCOG is often used to get the initial values for other retracking methods. The selection of threshold level for threshold method is critical. Table 1 shows that the threshold method performs best with 50% and 25%

threshold level for LRM and SARIn waveforms, respectively.

In the transect from Zhongshan Station to Dome A, the LRM and SARIn mode are adopted. The LRM is similar to the operation of conventional altimeters. SARIn mode is the combination of SAR and interferometry, which makes it possible to accurately determine the arrival direction of the echoes both along and across the satellite track. Figure 6 shows the waveform series for LRM and SARIn modes. The gate range is 0~127 for LRM mode and 0~511 for SARIn mode. The SARIn waveforms are much more intensive and complex than LRM waveforms, and the RMS of retracking distance correction is much larger than that of LRM waveforms.



(a)



(b)

Figure 6. Waveform series for LRM (a) and SARIn (b) modes

## 5. CONCLUSION

Satellite altimetry waveform retracking methods are discussed in the paper. Six retracking methods are used to retrack CryoSat-2 waveform over the transect from Zhongshan Station to Dome A. OCOG method uses all powers of waveform but has low precision. The linear  $5-\beta$  parametric method gives the best results for LRM and SARIn waveforms, but cannot make full use of the

waveform data. The threshold method is fit for the CryoSat-2 altimetry waveform retracking with the consideration of waveform retracking success rate and RMS of retracking distance corrections. The threshold method performs best with 50% and 25% threshold level for LRM and SARIn waveforms, respectively.

## ACKNOWLEDGEMENTS

This study is supported by the State Key Program of National Natural Science of China, No. 41531069; the Independent research project of Wuhan University, 2017, No. 2042017kf0209; the National Natural Science Foundation of China, No. 41176173; the Polar Environment Comprehensive Investigation and Assessment Programs of China, No. CHINARE2017.

## REFERENCES

- Anzehofer M, Shum C K, Rentsch M. 1999. Coastal altimetry and applications. Rep 464, Dept Geod Sci and Surveying, Ohio State University, Columbus.
- Bamber J L, Gomez-Dans J L, Griggs J A. 2009. A new 1 km digital elevation model of the Antarctic derived from combined satellite radar and laser data – Part 1: Data and methods. *The Cryosphere*, 3, pp. 101-111.
- Davis C H. 1997. A robust threshold retracking algorithm for measuring ice-sheet surface elevation change from satellite radar altimeter. *IEEE Transactions on Geoscience and Remote Sensing*, 33(5), pp. 1108-1116.
- Guo J Y, Hwang C W, Chang X T, et al. 2006. Improved threshold retracker for satellite altimeter waveform retracking over coastal sea. *Progress in Nature Science*, 16(7), pp. 732-738.
- Lee H, Shum C K, Emery W, et al. 2010. Validation of Jason-2 altimeter data by waveform retracking over California Coastal Ocean. *Marine Geodesy*, 33(S1), pp. 304-316.

Li F, Yuan L X, Zhang S K, et al. 2016. Mass change of the Antarctic Ice Sheet derived from ICESat laser altimetry. *Chinese J. Geophys.*, 59(1), pp. 93-100.

Martin T V, Zwally H J, Brenner A C, et al. 1983. Analysis and retracking of continental ice sheet radar altimeter waveforms. *Journal of Geophysical Research*, 88(C3), pp. 1608-1616.

Khaki M, Forootan E, Sharifi M A. 2014. Satellite radar altimetry waveform retracking over the Caspian Sea. *International Journal of Remote Sensing*, 35(17), pp. 6329-6356.

Wingham D J, Rapley C G, Griffiths H. 1986. New techniques in satellite altimetry tracking systems. *Proceedings of IGARSS'86 Symposium, Zurich*, pp. 1339-1344.

Wingham D J, Francis C R, Baker S, et al. 2006. CryoSat: A mission to determine the fluctuations in Earth's land and marine ice fields. *Advances in Space Research*, 37(4), pp. 841-871.

Yuan L X, Li F, Zhang S K, et al. A study of Arctic sea ice freeboard heights from ICESat/GLAS. *Geomatics and Information Science of Wuhan University*, 2016, 41(9), pp.1176-1182.

Zhang S K, E D C, Wang Z M, et al. 2007. Surface topography around the summit of Dome A, Antarctic, from real-time kinematic GPS. *Journal of Glaciology*. 53, pp. 159-160.

Zhang S K, E D C, Wang Z M, et al. 2008. Ice velocity from static GPS observations along the transect from Zhongshan station to Dome A, East Antarctica. *Annals of Glaciology*, 48, pp. 113-118.

Zhang S K, Xiao F, Li F, et al. DEM development and precision analysis in two local areas of Antarctica, using Cryosat-2 altimetry data. *Geomatics and Information Science of Wuhan University*, 2015, 40(11), pp.1434-1439.